Available online at www.sciencedirect.com
SCIENCE DIRECT®
Polymer 45 (2004) 3709–3720
polymer
www.elsevier.com/locate/polymer

Effect of ultrasound on thermoset polyurethane: NMR relaxation and diffusion measurements

Sayata Ghose[a], Avraam I. Isayev[a], Ernst von Meerwall[b,*]

[a]*Institute of Polymer Engineering, The University of Akron, Akron, OH 44325-0301, USA*
[b]*Departments of Physics, Chemistry and Polymer Science, The University of Akron, Akron, OH 44325-4001, USA*

Received 16 January 2004; received in revised form 17 March 2004; accepted 17 March 2004

Abstract

Recycling of rubber-based materials is of increasing industrial environmental importance. In order to characterize the effect of ultrasound on polymer networks, nuclear magnetic resonance (NMR) relaxation and pulsed-gradient diffusion measurements were made at 70.5 °C in polyurethane rubber (PUR) and foam after subsequent treatment by intense ultrasound. The proton transverse relaxation decay was analyzed in terms of molecular and segmental mobilities of all motional species, a chemical and physical network as well as diffusing sol. The diffusivity spectrum, measurable in foams, reflected the changing molecular weight distribution of low-molecular weight sol and oligomers. It was observed that the effect of ultrasound was less pronounced in PUR than rubbers like SBR, PDMS and BR owing to its low degree of unsaturation. The investigation on the foams is the first of its kind to be reported.

Keywords: Polyurethane; Ultrasound; Recycling

1. Introduction

Solid state nuclear magnetic resonance (NMR) has been used to study the molecular structure and dynamics of a large number of polymers including polyurethanes (PU). Typically, all polyurethanes consist of a hard segment from the diisocyanate and a soft segment from the polyol causing a phase separation via the segregation of these two components. Solid state NMR has been used to study the domain structure of the segmented PUs. Typical studies include the examination of microscopic dynamical properties of linear and crosslinked PUs [1]. These have shown that the differences between the hard and soft phase mobilities decrease with crosslinking, and the mobilities of the segments in separate domains are relatively independent of each other in a linear PU but are closely coupled in a crosslinked one. Techniques based on the Goldman–Shen pulse sequence have been used for studying the domain morphology by correlating relaxation times with molecular mobility and morphology [2]. The Thomson–Gibbs analysis has been applied to the temperature variations of the ^{1}H free induction decay (FID), when the mobility of the soft segments approaches that of the hard segments and the simple analysis of ^{1}H FID is not possible [3]. The transverse relaxation time of protons (^{1}H T_2) as well as cross-polarization time constant, T_{CH}, relate the NMR measurements to the mechanical properties and crosslink density of organic polymers, and have been studied for polyalkylene glycol (PAG) based PU acrylate coatings [4].

The recycling of waste rubbers is an important issue facing the rubber industry in recent years. In order to recycle waste rubber, it is necessary to break down its three-dimensional crosslinked structure in order to be able to revulcanize and reprocess it. One of the most promising methods for the devulcanization of rubber is the application of powerful ultrasound. Extensive studies have been carried out on various rubbers including ground tire rubber [5,6], natural rubber (NR) [7], ethylene–propylene diene rubber (EPDM) [8], styrene–butadiene rubber (SBR) [9], and poly(dimethylsiloxane) (PDMS; silicone rubber) [10,11].

Ultrasound degradation is known to involve severing of chemical crosslinks as well as some scission of the main

* Corresponding author. Address: Department of Polymer Science, The University of Akron, 170 University Avenue, Akron, OH 44325-3909, USA. Tel.: +1-330-972-5904; fax: +1-330-972-5290.
E-mail address: evm@physics.uakron.edu (E. von Meerwall).

0032-3861/$ - see front matter © 2004 Elsevier Ltd. All rights reserved.
doi:10.1016/j.polymer.2004.03.053

chains, in proportions favoring the weakest bonds, generally the crosslinks. In liquids intense ultrasound produces cavitation; the periodic collapse of the bubbles rapidly liberates localized thermomechanical energy available for bond rupture in molecules. In polymer melts and networks, the principal degradation mechanism is thought to involve transient cavitation in the likely absence of complete collapse; the resulting thermomechanical actions will lead to bond breakage in a manner resembling fatigue. Longer, less mobile, chains and segments are more susceptible to degradation than shorter ones, suggesting that over greater distances longitudinal wave components can produce force gradients sufficient for direct tensile rupture particularly at the weaker single bonds far from free chain ends.

The molecular mobility of ultrasonically devulcanized SBR has been studied using ^{13}C and ^{1}H NMR relaxation and ^{1}H pulsed-gradient spin-echo (PGSE) diffusion measurements [12,13]. It was reported that proton T_2 relaxation decay in devulcanized SBR consisted of two major components, attributed, respectively, to the extractable sol and the unextractable gel. On the other hand, the study of silicone rubber [14,15] and butadiene rubber (BR) [16] showed that transverse relaxation decay in both devulcanized BR and devulcanized silicone rubber consisted of three components. These were attributed to entangled and cross-linked networks; light sol and dangling network fragments; and oligomers including an unreactive trace.

In the present study, ultrasound decrosslinking has been applied to high-resiliency flexible polyurethane foams, a class of thermoset PUs as well as polyurethane rubber (PUR). In an effort to improve our understanding of the decrosslinking process in foam and the devulcanization process in rubber, a complementary study of the molecular mobility of the entanglement and crosslink network and the production, segmental mobility, and diffusion rate of the smaller sol molecules was undertaken. This investigation, reported here, was performed using ^{1}H NMR transverse relaxation and PGSE diffusion measurements.

2. Experimental

2.1. Materials

The PU foam used was high-resiliency flexible open-cell PU foam obtained from The Woodbridge Group in Troy, Michigan. Pore size has a narrow distribution in the range of several micrometers. The primary use of this foam is in the manufacture of automotive car seats. In the NMR experiments, the foams were easily compressed to about one-half their original volume, in order to increase the filling factor and hence the spin signal.

The PUR used for the experiments is Vibrathane 5008, a polyester-based PUR with a M_w close to 70,000 and made by Uniroyal Chemical Company.

2.2. Ultrasound reactor

The foam was fed into a grooved barrel reactor [17]. In this reactor, two ultrasonic horns of rectangular cross-section (38.1×38.1 mm) are inserted into the barrel through two ports. The axes of the horns are perpendicular to the barrel and thus allow the imposition of longitudinal waves perpendicular to the flow direction. In order to build up sufficient die pressure at the exit of the extruder, the die used for extrusion had a diameter of 58.42 mm, tapering down at an angle of 21.8° to a diameter of 11.68 mm. The temperature of the extruder was set at 120 °C, and the screw speeds were 20 and 50 rpm. The material was very difficult to feed and was fed manually after cutting it into pieces approximately 3×3 cm. The output feed rate varied between 13.5 and 15.5 g/min, with a lower feed rate for the untreated sample. Because of insufficient depth of the screw channel in the feeding zone, there was no significant difference in feed rates for the different screw speeds. The gap size was 2 mm, and ultrasound amplitudes at the transducer face of 5, 7.5 and 10 μm were used.

The coaxial devulcanization reactor used in the experiments with PUR consisted of a 38.1 mm single screw rubber extruder with the $L/D = 11$ and a coaxial ultrasonic die attachment [18]. Two barrel temperatures, 80 and 120 °C, and a screw speed of 20 rpm were used for the experiments. The gap sizes were kept at 2.5 and 3.0 mm, and a feed rate of 1.26 g/s was used. The experiments were carried out at amplitudes of 5, 7.5 and 10 μm.

2.3. Characterization

Both the decrosslinked foam and the devulcanized rubber were collected and homogenized on the two-roll mill (Dependable Rubber Machinery, Cleveland OH). Gel fraction and crosslink density were determined by the Soxhlet extraction method using THF as the solvent. The extraction time was 24 h. After 24 h, the weight of the swollen sample was measured after removing the surface solvent. Then the samples were dried in an oven at 65 °C for 24 h, and allowed to stand at room temperature before the weight was taken again. Crosslink density was calculated using the Flory–Rehner equation [19]. Molecular weight measurements were carried out using a Waters 410 Differential Refractometer. THF solvent was run at room temperature; conventional calibration was used against polystyrene standards.

2.4. NMR experiments

All NMR and diffusion measurements were conducted in the ^{1}H resonance at 70.5 °C. The elevated temperature was chosen to accelerate molecular/segmental motions and enhance differences between gel and sol in the samples. The 33 MHz modified Spin–Lock CPS-2 spectrometer, equipped with attachments to permit diffusion measurements,

and the data interpretation methods have been comprehensively described elsewhere [14,20–22]. The pulse sequence employed for the relaxation experiments was the standard principal Hahn two-pulse sequence on resonance, 90°-τ − 180°-τ—echo, while for the PGSE experiments the stimulated spin echo sequence 90°-τ_1 − 90°-τ_2 − 90°-τ_1—echo was used off-resonance. The pulse spacing τ in the T_2 experiments was adjusted from 0 to at least 15 ms in 25 or more steps, until the signal-to-noise ratio fell below 0.2% of its initial value.

In case of PUR, the NMR T_2 measurements were also conducted in the ^{1}H resonance at 70.5 °C. At this temperature, none of the samples provided an opportunity for performing diffusion measurements as a result of their more rapid transverse relaxation decay. The situation was no different when the experiments were tried at a higher temperature of 100 °C. Since it was desirable to compare results with our previous NMR studies carried out with other types of rubber conducted at 70.5 °C, the experiments were done at this temperature.

The non-spectroscopic PGSE experiments were performed at a fixed magnitude of the pulsed magnetic field gradient, G, by varying the duration δ of each of the pair of gradient pulses coordinated with the stimulated-echo radio frequency (rf) pulse sequence. In this work, the rf pulse spacing, τ_1, between the first two 90° pulses was 12 ms, and the spacing $\tau_1 + \tau_2$ between the first and third pulses, hence also the spacing Δ between the gradient pulses, was 70 ms. To minimize residual gradient effects, δ was never larger than $\Delta - 6$ ms, but usually did not exceed 3 ms. For diffusing molecular species the echo is attenuated; its amplitude is recorded as function of the gradient parameter $X = \delta^2 G^2(\Delta - \delta/3)$, where the delay between the gradient pulses is $\Delta = \tau_1 + \tau_2$. To ensure stability and convenient access to the echo signal baseline, a small steady gradient of magnitude, G_0, was applied throughout, and this required the addition to X of a small term, proportional to GG_0. In this study, fixed values of $G = 634$ Gauss/cm and $G_0 = 0.3$ Gauss/cm were used, and δ was varied from eight to 12 steps until the echo signal was attenuated to the background noise level, or until $\delta = 12$ ms was reached. Signal averaging between 5 and 12 passes for each δ, improved the signal-to-noise ratio. Experiments were conducted off-resonance by −3 kHz in single-sideband mode with single-phase rf phase-sensitive detection, and the echo signal A was measured as the integral over the magnitude Fourier transform of the beat between echo and reference, after correction for *rms* baseline noise. Several independent checks revealed no explicit dependence of the extracted diffusion coefficient on Δ, ensuring that the diffusion was Fickian.

The objective of these combined procedures was to ensure the characterization of the tail of the echo decay, from which light sol fraction and sol mobility are inferred. It further ensured that the initial, rapid T_2 decay, arising from non-diffusing physical or chemical network, did not interfere with the measurement of sol or oligomer diffusion. Optimization of magnetic field homogeneity combined with the low sol diffusion coefficient (shown below) confirmed that the T_2 values measured with the two-pulse sequence were not falsified by diffusional artifacts [23].

2.5. T_2 Data analysis

In previous work, [14–16] the echo decay had been analyzed in terms of a three-component relaxation model as the initial two-component model proved unsatisfactory in many cases. The final model, employed here successfully in all cases, is given by

$$\frac{A(2\tau)}{A(0)} = f_S \exp(-2\tau_1/T_{2S})^E + f_L \exp(-2\tau_1/T_{2L}) + (1 - f_S - f_L)\exp(-2\tau_1/T_{2M}), \quad (1)$$

where T_{2S}, T_{2M}, and T_{2L} signify the short, medium, and long relaxation times, respectively; f_S, $(1 - f_S - f_L)$, and f_L are their relative intensities; and E is the Weibull exponent describing the departure of the fastest decay from exponentiality.

When the diffusion of light sol is to be studied, this can conveniently be done provided $T_{2L} \gg T_{2S}$, as was the case in this study, simply by operating near the optimal condition:

$$T_{2S} \ll 2\tau_1 \leq T_{2L} \text{ (max. sol echo, no gel echo)} \quad (2)$$

This procedure resulted here in the choice of $\tau_1 + \tau_2 = 70$ ms for decrosslinked samples at $T = 70.5$ °C, and ensured that our diffusion measurements were free of distortion by echo contributions from the gel.

2.6. PGSE Data analysis

In the non-spectroscopic high-gradient version of the PGSE method employed in all cases such as the present one, where chemical shift differences are unresolvable, a D distribution manifests itself as an upward concavity in the echo attenuation plots $\log A$ vs. X, arising from a linear superposition of component attenuations [20]. When the diffusion rates are expected to display an arbitrary distribution, the rates may be modeled as several components having fractional amplitudes a_i and diffusion coefficients D_i; thus the echo attenuation assumes the form

$$\frac{A(2\tau, X)}{A(2\tau, 0)} = \sum_i a_i \exp(-\gamma^2 D_i X), \quad (3)$$

where γ represents the gyromagnetic ratio of the nucleus at resonance (^{1}H).

For a system consisting of only two diffusing specimens, Eq. (3) can be written as

$$\frac{A(2\tau, X)}{A(2\tau, 0)} = f_{fast} \exp[-\gamma^2 D_{fast} X] + (1 - f_{fast})\exp[-\gamma^2 D_{slow} X], \quad (4)$$

where D_{fast} and D_{slow} represent the diffusion of the two

species and f_{fast} denotes the echo fraction of the fast-diffusing species at $t = 2\tau_1 + \tau_2$. When one component (usually the slower-diffusing species) displays a diffusivity distribution that arises from molecular polydispersity, the second component is modeled in terms of Eq. (3) with a_i and D_i based on the known M-distribution and the scaling relation (Rouse or reptation) between molecular weight and diffusion. The polydispersity value (M_w/M_n) is provided as input and is kept fixed. The adjustable parameters are D_{fast}, $D(M_n)$, (the mean diffusion rate of the slow-moving species), and f_{fast}.

3. Results and discussion

3.1. PU foams

Fig. 1 shows the transverse relaxation–decay plot analyzed in terms of a two-component relaxation model for PU foam treated at a gap of 2 mm and an amplitude of 5 μm. As is evident from the figure, this is not a good fit; the chi-square nu (χ^2_ν) value of 14.9, a measure of the goodness of fit, is unacceptably high. To guide the further analysis, the data was subjected to an inversion in terms of 40 components; Fig. 2 shows the result for a foam treated at a gap of 2 mm and an amplitude of 10 μm. This spectral decomposition (component amplitude vs. log of the relaxation time) shows a wide distribution of decay rates which can be broadly classified into three groups, discrete fast and slow relaxations each separated from a range of intermediate rates. The χ^2_ν value is reduced to 1.29, indicating a reasonable fit, far better than the two-component model. Thus, the final analysis approximated this distribution in terms of three components. Fig. 3 shows the transverse relaxation decay data analyzed in terms of the six-parameter model of Eq. (1). In most cases the χ^2_ν value is further reduced. This approach represented an economical compromise between goodness of fit and number of adjustable parameters.

Fig. 4 shows a plot of the chemically extracted sol fraction vs. ultrasound amplitude during the treatment of the foam. It is seen that the amount of sol increases sharply with increase in amplitude, indicating that more sol is being formed when the conditions of treatment become more severe. Fig. 5 shows T_{2S}, T_{2M} and T_{2L} plotted as a function of the fraction of sol, the latter representing a measure of the extent of decrosslinking. It is observed from the figure that the molecular mobilities of all the components increase with increase in ultrasound exposure. This phenomenon represents a sol-induced increase in the mobility of the network.

This information, in terms of f_S, f_L and $f_M = (1 - f_S - f_L)$ is shown in Fig. 6 as a function of the fraction of extractable sol. The bold line in the figure represents the extractable sol fraction itself; its position lies well above f_L, indicating that a portion of the intermediate and perhaps even the short component arises from the chemically extractable material. However, the fact that $f_L + f_M$ exceeds the extractable sol fraction is an indication that the remaining portion of the intermediate component, as well as all, or almost all, of the short component, arises from the material that could not be extracted. This means that the

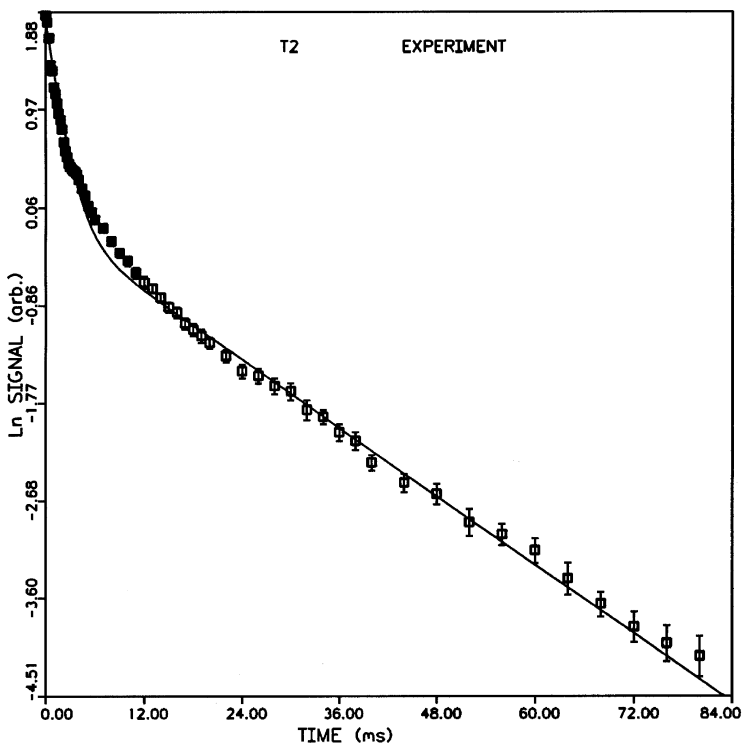

Fig. 1. Transverse proton relaxation decay at 70.5 °C of PU foam, treated at a gap of 2 mm and an amplitude of 5 μm, analyzed using a two-component model.

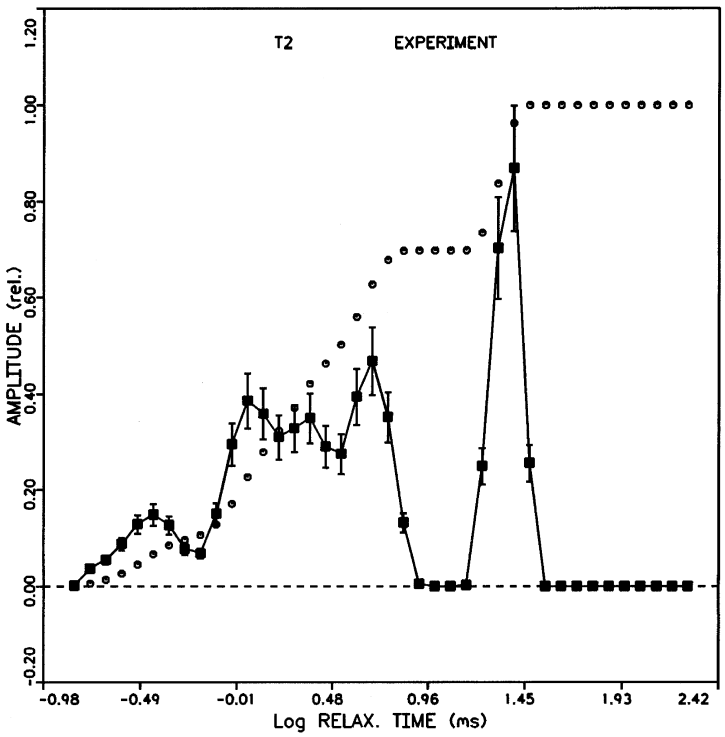

Fig. 2. Spectral decomposition (40 components) of the transverse magnetization decay of foam treated at a gap of 2 mm and an amplitude of 10 μm.

intermediate component must consist of some sol and some dangling ends in the network. In previous studies involving unfilled silicone [14] and butadiene [16] rubber, it was seen that the portion of intermediate component increased with an increase in sol fraction. In the present case of PU foam, the intermediate fraction remains virtually constant.

Based on the component mobilities and their relative contributions and their dependence on the sol fraction, we may assign the short component to the crosslinked and highly entangled network, loosened and diminished with increase in ultrasound treatment and penetrated by the highly mobile and diffusing sol. The unreactive oligomers that are always present irrespective of the nature of the treatment can be recognized as the long component. This component may also include some small amounts of light, unbranched material that may have been generated by the ultrasound treatment. It appears that ultrasound exposure of PU foam degrades the network by detaching molecular fragments of at least intermediate size, but leaves substantial amounts of dangling fragments. Significantly, ultrasound seems inefficient at further tearing such fragments into oligomeric dimensions, or detaching oligomer-size material directly from the network. This observation is in accord with the results obtained from literature [24–26] related to the effects of ultrasound on polymers in solution indicating a certain limiting molecular weight is achieved under ultrasound treatment (about 30,000 for polystyrene).

The molecular weight (M_n and M_w) and the polydispersity of the sol extracted from the untreated and treated foams are shown in Fig. 7 as a function of the ultrasound amplitude. Clearly, the polydispersity index increases slightly upon treatment. The analysis of the PGSE data was modeled based on these values. Fig. 8 shows an example of diffusional echo attenuation data for foam decrosslinked at an amplitude of 10 μm, together with a fit of Eq. (4); reptational scaling was invoked as the slowly-diffusing component could safely be assumed to be entangled. There was complete echo attenuation, as is evident by the absence of the approach of the echo amplitude to a horizontal asymptote. The diffusional entanglement onset molecular weight (M_c) for linear PU is 7 kg/mol [27]. An echo signal from the short T_2 component ($T_{2S} \leq 1$ ms), consisting of the crosslinked and the highly entangled species (molecular weight greater than 3–10 times the value of M_c), is totally absent in the diffusion studies, conducted at $\tau_1 = 12$ ms. Only the oligomeric and most of the detached, unentangled fragments (with molecular weight less than 3–10 times the value of M_c), consisting of intermediate and long T_2 were available for diffusion studies. At a temperature of 70.5 °C, only the treated foam samples provided an opportunity for performing diffusion measurements as a result of their higher long-T_2 fractions. Fig. 8 suggests that the fast-diffusing portion arises from the oligomeric species that relax at T_{2L}, and the slower-diffusing species is from the slightly entangled (molecular weight less than 3–10 M_c) molecular fragments.

Fig. 9 shows the diffusivities, D_{fast} and $D(M_n)$, plotted as a function of the extracted sol. At lower sol fraction, the two rates differ by almost two orders of magnitude, but this difference decreases with increase in sol; the decrease of

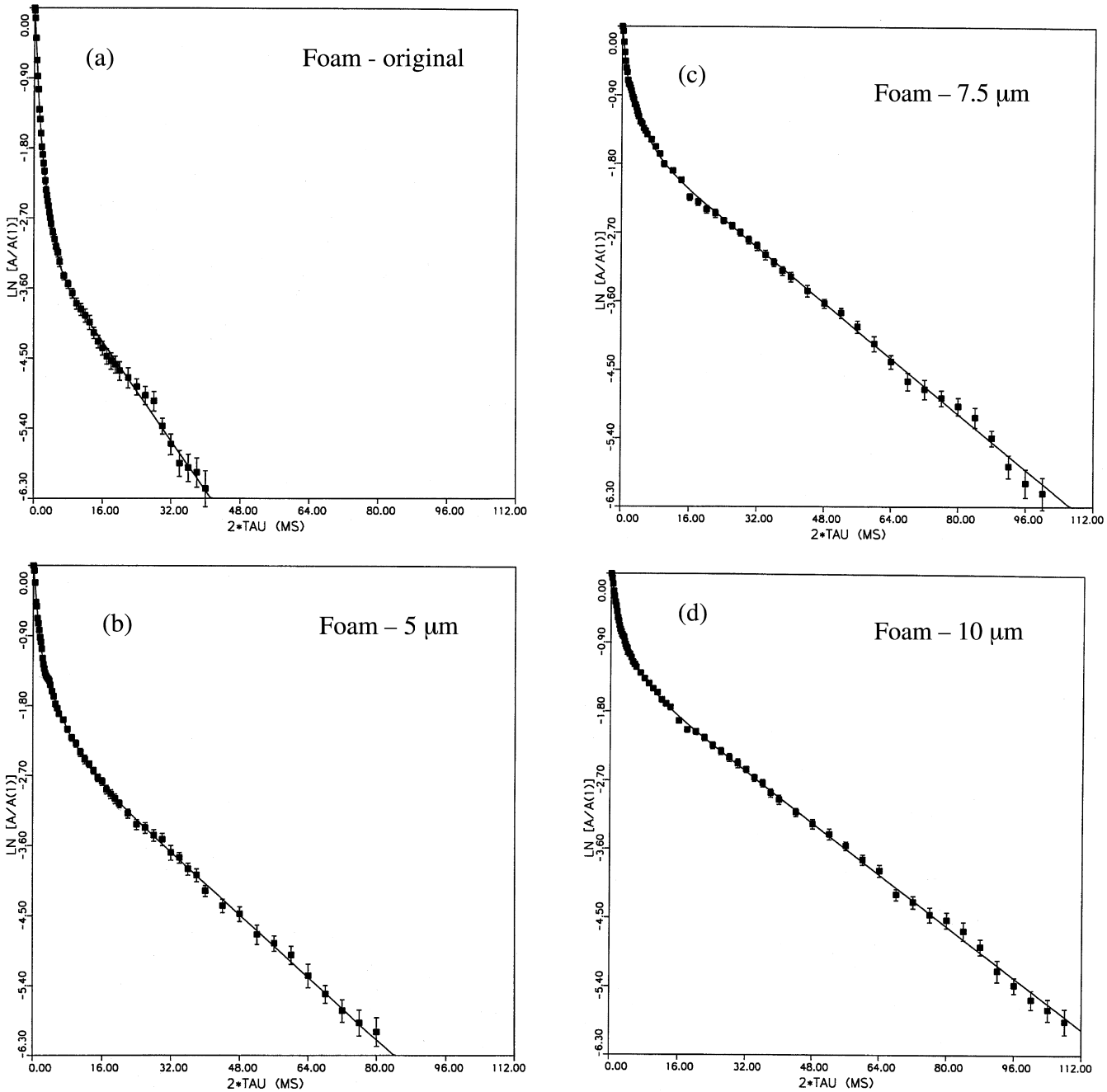

Fig. 3. Transverse proton magnetization decay in PU foam: untreated (a) and 5 μm treated (b) PU foam with a three-component, six-parameter fit of Eq. (1). Transverse proton magnetization decay of 7.5 (c) and 10 μm (d) treated PU foam with a three-component, six-parameter fit of Eq. (1).

diffusivities of the fast-moving species is greater than that of the slow-moving species. This observation is taken to indicate that with treatment the mean molecular weight of the fast moving species is increasing, i.e. low-molecular-weight polymers are being formed adding to the initial amount of oligomers. The increasing T_2 values support the notion that the treated samples contain more midsize components in the fast-moving fraction, hence lowering the mean fast-diffusion coefficient. The diffusion coefficients of the slow-moving species are relatively unchanged with treatment, indicating that the relative proportions of the higher molecular weight fractions of the diffusing sol do not change.

From the diffusion data, additional information regarding the fractional contribution of the fast-diffusing portion of the echo (f_{fast}) may be obtained. Fig. 10 shows that this value increases with increase in the extractable sol, but this result may mislead as τ_1 was kept the same for all the diffusion experiments whereas the components' relaxation times and their relative amplitudes and hence, their contribution to the echo ($2\tau_1 = 24$ ms), varied systematically. In order to obtain the proportion of the fast-moving species, F_{fast},

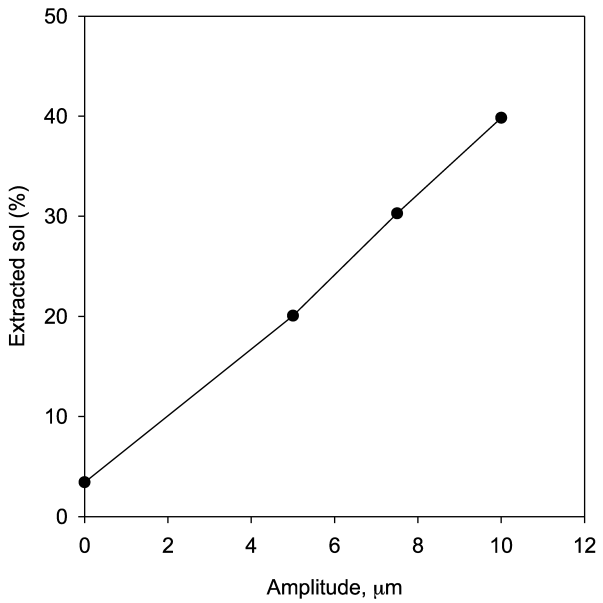

Fig. 4. Extracted sol (%) vs. amplitude for untreated and treated PU foam, the condition of treatment being a screw speed of 20 rpm, a barrel temperature of 120 °C, a gap size of 2 mm and various amplitudes.

present in the sample (rather than merely in the echo signal), the results of the T_2 and diffusion experiments must be combined [14]. For this purpose f_L is augmented by a T_2-weighted portion of f_M, as follows [15]:

$$F_{\text{fast}} = f_{\text{fast}}(2\tau_1) f'_L(2\tau_1) \tag{5}$$

with

$$f'_L(2\tau_1) = f_L + f_M \exp[2\tau_1(T_{2L}^{-1} - T_{2M}^{-1})]. \tag{6}$$

It is seen from Fig. 10 that although the sol fraction

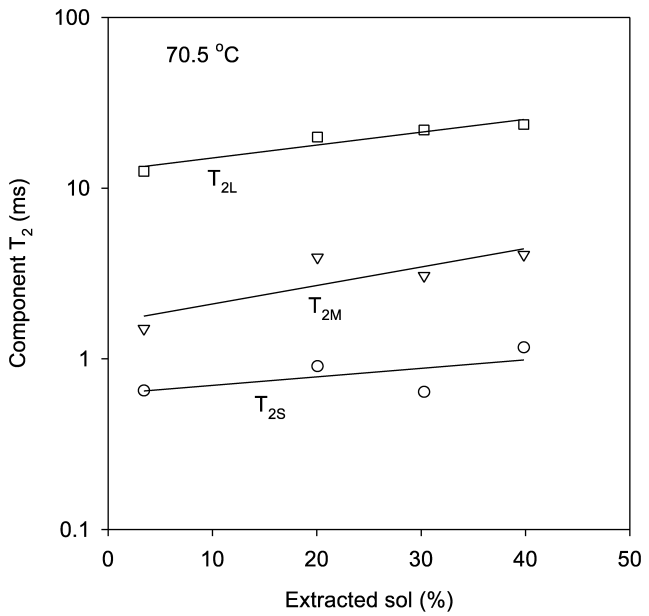

Fig. 5. T_2 relaxation times of short, medium and long components for untreated and treated foams as a function of extractable sol content.

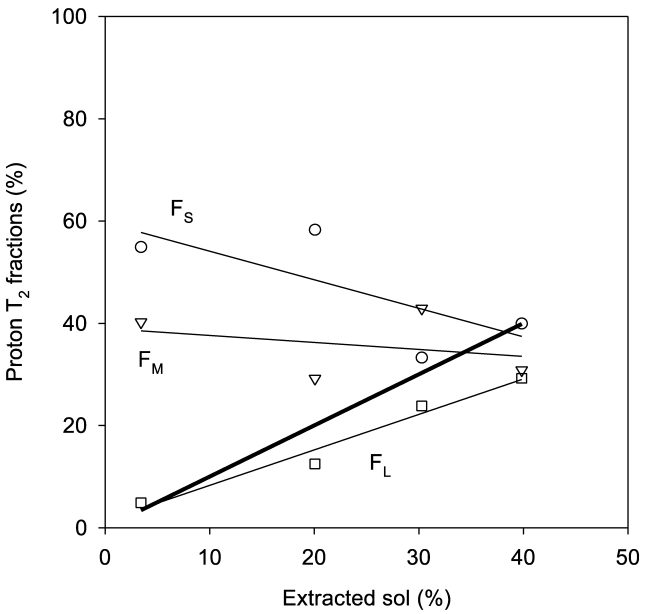

Fig. 6. Fraction of short, medium and long components for untreated and treated foams as a function of extractable sol content.

increases to 40% as a result of the treatment, the fraction of the sample diffusing at the highest rates increases to only 6%. From Figs. 6 and 10 it may be inferred that F_{fast}, related to f_L, includes the unreactive oligomers that are present in the sample for all specimens irrespective of treatment.

Changes in the diffusion coefficient may arise from one or more of three separate causes: changes in the diffusant's average molecular weight; changes in host molecular mobility, e.g. by free volume; and changes in diffusant/host monomeric friction constant at constant free volume, e.g. due to branching. Unlike SBR [13], the glass transition

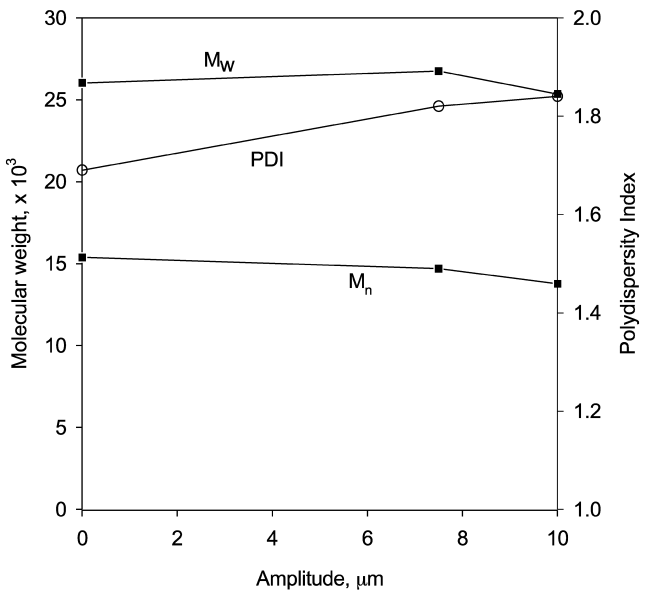

Fig. 7. Molecular weight (solid symbols) and polydispersity index (open symbols) of untreated and treated foams as a function of ultrasound amplitude.

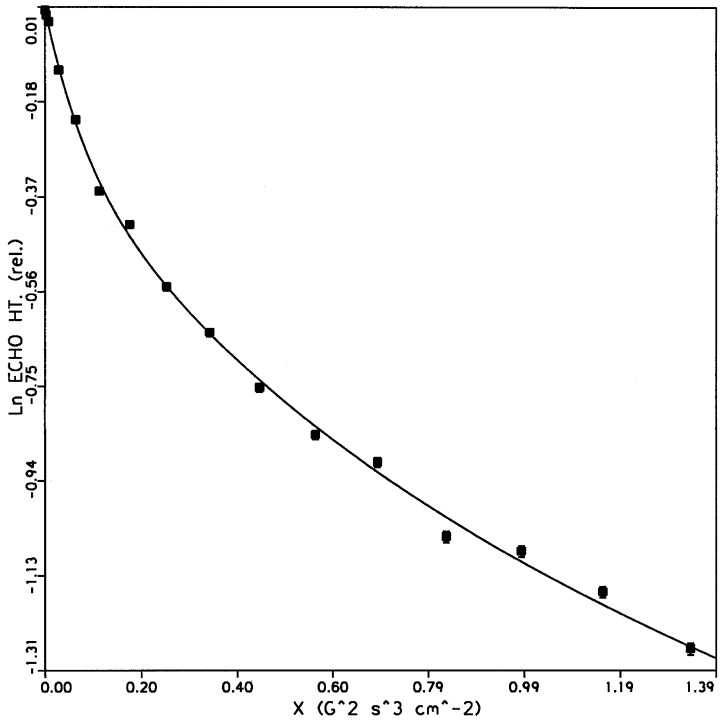

Fig. 8. Diffusion spin-echo attenuation in PU foam decrosslinked at a screw speed of 20 rpm, a barrel temperature of 120 °C, a gap size of 2 mm and an amplitude of 10 μm.

temperature measured in untreated and treated PU foam specimens was not sensitively dependent on ultrasound exposure (Fig. 11), thereby ruling out any substantial free-volume-based diffusivity changes. Again, the effects of molecular weight and of branching in the light sol molecules produced by ultrasound are not separable in the present experiment. Although significant differences are observed in the T_2 experiments, there does not seem to be a noticeable change in mean diffusivity of the slow-moving species with change in condition of treatment. Thus, the decrease of D_{fast} with treatment confirms that low-molecular-weight polymers may be forming to augment the oligomers present initially in the samples, increasing the mean molecular weight of the fast-diffusing fraction.

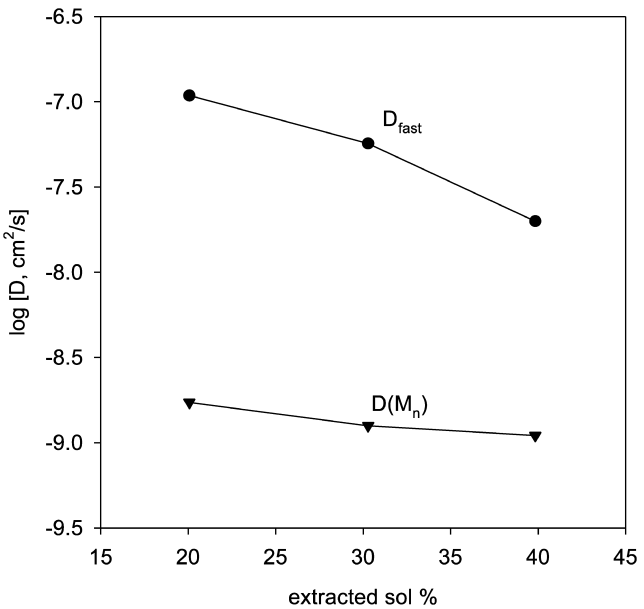

Fig. 9. Diffusion coefficient of the fast component and the mean diffusion coefficient of the slow component for foams treated at various amplitudes plotted against the extracted sol %.

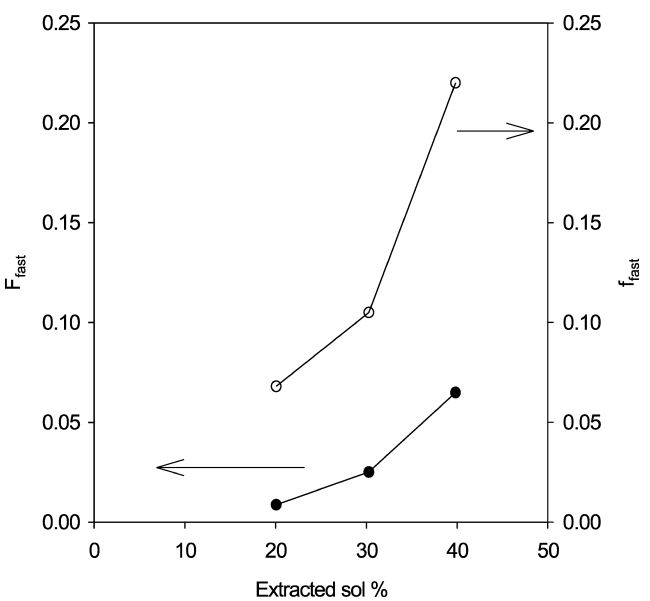

Fig. 10. Contribution of the fast-diffusing portion of the echo (f_{fast}, open symbols) and fast-diffusing species of the sample (F_{fast}, solid symbols.

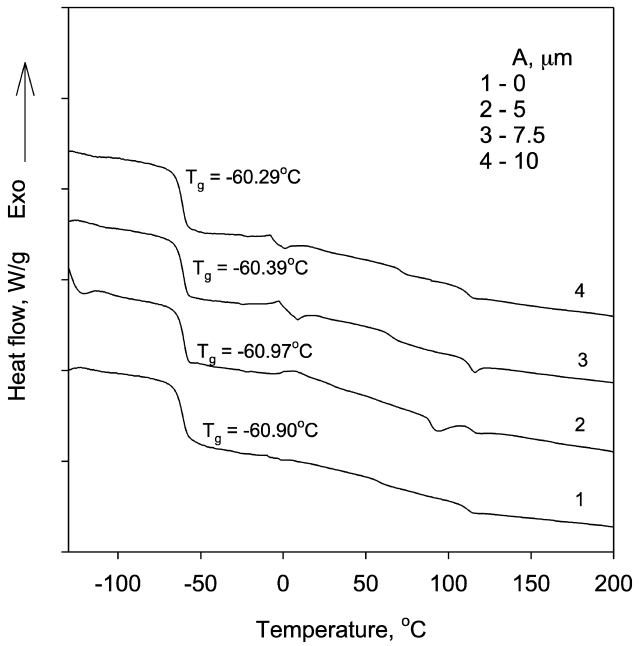

Fig. 11. Glass transition temperatures for untreated and treated foams.

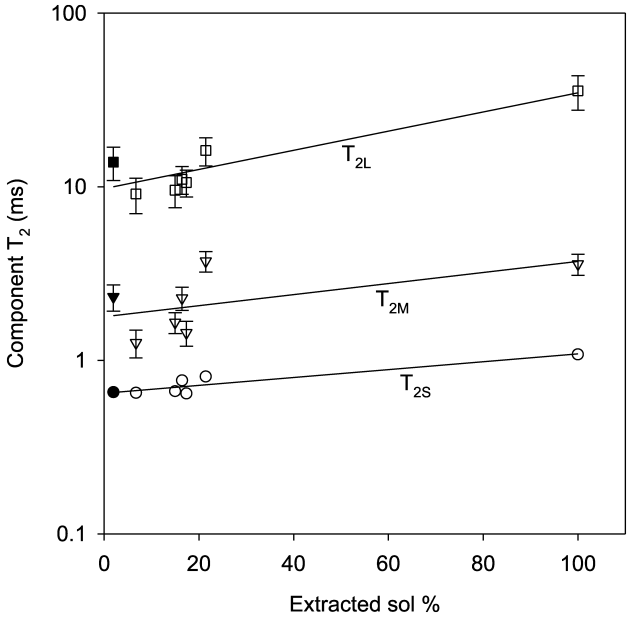

Fig. 13. T_2 relaxation times of short, medium and long components for gum, vulcanized (solid symbols) and treated PUR as a function of extracted sol.

3.2. PU rubber

Transverse relaxation measurements were performed in all rubber specimens as described above. The analysis of the data, too, proceeded along the same lines as for the foams, with similar results: the three-component model of Eq. (1) again proved to be an optimal description of all data.

Fig. 12 shows the transverse relaxation decay data of the vulcanized gum, analyzed in terms of Eq. (1). Fig. 13 shows T_{2S}, T_{2M} and T_{2L} for all PUR specimens as a function of the fraction of sol, the latter again representing a measure of the extent of devulcanization. It is evident that the molecular mobilities of all the components increase with increase in ultrasound exposure. The amount of increase is similar in all three cases, indicating that the mobilities of all the three components are affected to the same extent. The observation

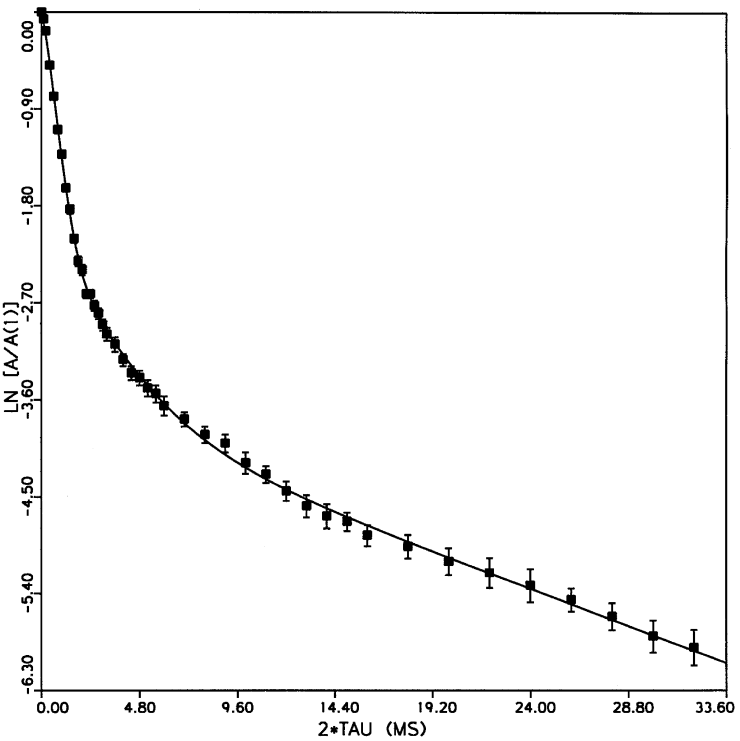

Fig. 12. Transverse proton magnetization decay of vulcanized PUR with a reasonable three-component, six-parameter fit of Eq. (1).

that T_{2S} shares in this increase represents a sol-induced enhancement of the mobility of the network. The less tightly linked the network structure, the greater is the mobility, with the gum showing the highest mobility.

Additional information is contained in the relative component intensities f_S, f_L and $f_M = (1 - f_S - f_L)$, shown is Fig. 14 as function of the fraction of extractable sol. The bold line represents the extractable sol fraction itself. Its position lies well above f_L, again indicates that a portion, but not all, of the intermediate and perhaps even the short component arises from the chemically extractable material. The amount of f_L remains unchanged while f_M shows a slight decrease; the experimental uncertainties suggest that this change is not significant. The assignment of the three relaxation components to network, sol plus dangling ends, and oligomers remains the same as in the case of the foams.

It is evident that the effect of ultrasound treatment on segmental mobility on PUR is weaker than on PU foam and rubbers such as SBR [13], PDMS [14] and BR [16]. In all the materials studied so far it has been found that ultrasound detaches, from the crosslinked network, fragments of at least intermediate size. In the present case, it appears that ultrasound exposure degrades the network by detaching molecular fragments of size so substantial that they have molecular mobilities similar to the untreated network. Figs. 13 and 14 indicate that the mobilities of the vulcanized, treated, and gum samples are very similar. It should be remembered that wide-line NMR is not able to distinguish between highly entangled and crosslinked species; the present experiment cannot determine conclusively the extent of crosslink breakage and entanglement in the treated samples.

This fact that ultrasound detaches from the network

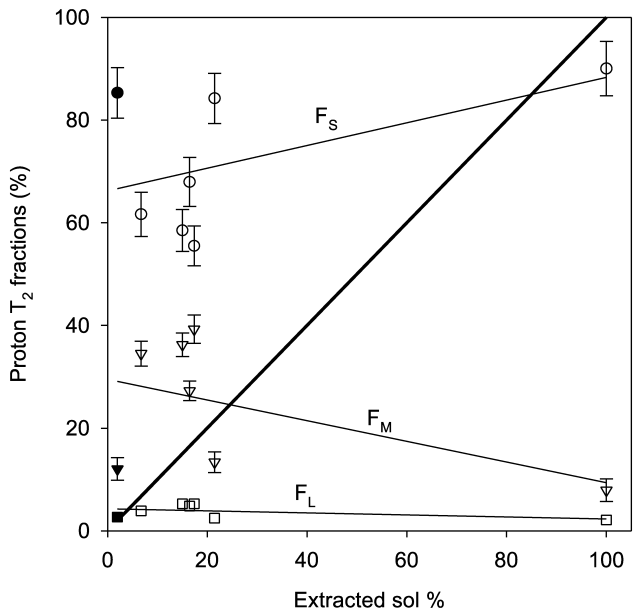

Fig. 14. Fraction of short, medium and long components for gum, vulcanized (solid symbols) and treated PUR as a function of extractable sol content.

highly entangled species is corroborated by the molecular weight data obtained from GPC measurements on the extracted sol. The diffusional entanglement onset molecular weight (M_c) for linear PU is approximately 7 kg/mol [27]. The molecular weight data for the gum, and for the sol in treated samples, are given in Table 1. As evident from the values, M_w of the sol is higher than 3 M_c, indicating that the sol contains highly entangled species. Thus whereas ultrasound is effective in breaking up the crosslinked network, it is ineffective in generating short, unentangled species. The reason for our inability to make diffusion measurements in PUR is attributable to the fact that whereas the component T_2 values are very similar to those in PU foams, the component intensities differ greatly: measurable diffusional echo attenuation depends on a substantial value of f_L, which in PUR never rises above 0.04. Measurements of T_g of the treated and untreated samples have shown no significant differences ($T_g = -16.7$ and -14.5 °C for untreated gum and vulcanizate, respectively, with a variation within 1 °C for the treated samples), indicating that there is no change in free volume taking place. Free volume is significantly enhanced by chain ends, and its increase would indicate the production of low molecular weights. Its constancy here confirms the results of the NMR experiments to the effect that mainly highly entangled species are being generated.

4. Summary and conclusions

This study of PU foam and PUR samples, using ^{1}H NMR transverse relaxation and PSGE diffusion measurements, complements the earlier NMR relaxation and diffusion study of the ultrasound devulcanization of SBR, silicone rubber and BR. The T_2 relaxation and diffusion rates of the PU foam samples and only the T_2 relaxation of the PUR were obtained. The transverse relaxation decay was successfully described in both cases using a three-component model, while the diffusivity spectrum for treated PU foams was bimodal in nature. The following conclusions can be drawn from the experiments:

(i) Based on the component mobilities obtained from the T_2 measurements, their relative contributions, and their dependence on the sol fraction, unreactive oligomers are recognized as the origins of the long components, and the short components are assigned to the highly entangled or crosslinked network in PU foam and PUR. The intermediate components must arise from sol of moderate molecular weight and from dangling network ends of similar mobility.

(ii) As a result of the treatment, the molecular mobilities of all the three fractions increase by comparable factors, with sol diffusion responsible for enhancing the segmental mobility of the network PU foam and PUR. This phenomenon has also been observed in previous experiments involving silicone rubber and BR.

Table 1
GPC data of gum and devulcanized PUR

Sample	M_n	M_w	PDI of main peak
Gum	42,300	65,100	1.54
1.26 g/s—2.5 mm gap—10 μm (sol part)	20,300	27,400	1.34
1.26 g/s—3 mm gap—10 μm (sol part)	22,500	32,600	1.45

(iii) In PU foams, the intermediate fraction remains virtually constant, accompanied by a trade-off between short and long component contributions. Ultrasound is less effective than in other rubbers in producing sol of intermediate sizes; in previous studies involving unfilled silicone and butadiene rubber the proportion of intermediate component increased with an increase in sol fraction.
(iv) In PU foams, ultrasound can detach molecular fragments of at least intermediate size but is less efficient at tearing the network into fragments of oligomeric dimensions. This observation recapitulates the results for other rubbers examined previously.
(v) The diffusivity spectrum for treated PU foams is bimodal in nature, separable into contributions from any fast-moving species and a slow-moving polydisperse species. The fast-diffusing portion arises mainly from oligomers that relax at T_{2L} and from newly detached light sol; the slower-diffusing species originates in unentangled and slightly entangled (molecular weight less than $3-10\,M_c$) molecular fragments.
(vi) $D(M_n)$ remains virtually unchanged with treatment, indicating that the molecular weight distribution of the bulk of the sol remains unaffected in PU foam. The decrease of D_{fast} is significant, indicating that with treatment some low-molecular weight polymers are being formed, adding to the initial amount of the faster-diffusing oligomers.
(vii) The behavior of PUR is different from the other rubbers or the PU foam. The presence of a significant f_S in the gum rubber indicates that it contains a substantial amount of entanglements which have short T_2. The amount of f_L remains unchanged while f_M shows a slight decrease.
(viii) The effect of ultrasound treatment on segmental mobility in PUR is weaker than in other rubbers studied. Ultrasound exposure degrades the PUR network by detaching molecular fragments of substantial size, which have molecular mobilities similar to the untreated network. But it is quite ineffective in generating short, unentangled species with higher mobilities.

The recycling of thermoset polyurethane by the application of powerful ultrasound is a novel approach in preparing for reprocessing this rubber. Since the incineration of PU evolves poisonous fumes of CO and HCN, the ultrasound method capable of breaking down the chemical crosslinks, is environment-friendly and safe. However, for any process it is important to know the probable mechanism. It is to this end that PGSE NMR plays a significant role. The results of the NMR relaxation and diffusion experiments reveal certain crucial effects of ultrasound on the crosslinked structure of thermoset PU. Chain/crosslink breakage occurs to yield fragments of various mobilities and sizes, a fact that can be related to the molecular data obtained from GPC measurements. Similar NMR experiments have been carried out with various rubbers like SBR, silicone rubber and BR but the results for PU differ significantly from these rubbers. PUR, having a low degree of unsaturation, seems to be less affected by ultrasound than other rubbers. This is evident from the fact that the molecular fragments detached from the PUR network exposed to ultrasound are of a size greater than was observed in other rubbers. The investigation on the foams is the first of its kind to be reported. Standard literature [28] states that crosslinking in polyurethane foams primarily consists of strong H-bonding of the urea groups, while chain extension takes place via the component functionality. Here the observed behavior in our experiments is similar to that in other rubbers.

The NMR studies in this paper provide a unique insight into the molecular mechanism of devulcanization of crosslinked PU. Investigations of ultrasound devulcanization of other polymer networks of industrial use, both unfilled and particulate filled, are in progress in this laboratory, employing similar combinations of NMR and diffusion measurements.

Once ultrasound-based recycling of industrial rubbers is fully developed, it is expected to be entirely competitive with other methods in current use. It is now known to be applicable to a variety of unfilled and filled rubbers with a minimum of adjustments, and offers major advantages in the degree to which revulcanization is able to recover the properties of the original material. The practicality of rubber recycling by any method is, of course, an economic issue, but consideration of past and current trends firmly suggests the likelihood of its increasing attractiveness to the most important rubbery materials, including those based on PU. Decrosslinking thermoset PU foams is of substantial interest since the sonicated output is easily converted into flowable form for blending with rubbery or thermoplastic PU to make useful products from materials otherwise requiring disposal.

Acknowledgements

This study was supported in part by Grant DMI-00-84740 from the US National Science Foundation.

References

[1] Assink RA, Wilkes GI. J Appl Polym Sci 1981;26:3689.
[2] Idiyatullin DS, Khozina EV, Smirnov VS. Solid State Nucl. Magn. Reson 1996; 7:17.
[3] Clayden NJ, Nijs CL, Eeckhaut GJ. Polymer 1997;38(5):1011.
[4] Youngman RE, Schissel DN, Gasper SM. Polym Prepr 2003;44(1): 350.
[5] Yun J, Oh JS, Isayev AI. Rubber Chem Technol 2001;74:317.
[6] Tukachinsky A, Schworm D, Isayev AI. Rubber Chem Technol 1996; 69:92.
[7] Tapale M, Isayev AI. J Appl Polym Sci; 1998;70:2007.
[8] Yun J, Isayev AI. Rubber Chem Technol 2003;76:253. Gummi Fasern Kunstoff, 2002;10:628.
[9] Isayev AI, Kim SH, Levin VY. Rubber Chem Technol 1997;70:194.
[10] Shim SE, Isayev AI. Rubber Chem Technol 2001;74:303.
[11] Diao B, Isayev AI, Levin VY. Rubber Chem Technol 1999;72:152.
[12] Levin VY, Kim SH, Isayev AI, Massey J, von Meerwall E. Rubber Chem Technol 1996;69:104.
[13] Johnston ST, Massey J, von Meerwall E, Kim SH, Levin VY, Isayev AI. Rubber Chem Technol 1997;70:183.
[14] Shim SE, Parr JC, von Meerwall E, Isayev AI. J Phys Chem B 2002; 106:12072.
[15] Shim SE, Parr JC, von Meerwall E, Isayev AI. J Polym Sci, Part B: Polym Phys 2003;41:454.
[16] Oh JS, Isayev AI, von Meerwall E. Rubber Chem. & Technol. Submitted for publication.
[17] Yun J, Isayev AI. Polym Engng Sci 2003;43:809.
[18] Tukachinsky A, Schworm D, Isayev AI. Rubber Chem Technol 1996; 69:92.
[19] Flory PJ, Rehner Jr J. J Chem Phys 1943;11:512.
[20] von Meerwall E, Ferguson RD. J Appl Polym Sci 1979;23:877.
[21] von Meerwall E, Palunas P. J Polym Sci, Part B: Polym Phys 1987;(7): 1439.
[22] von Meerwall E, Ferguson RD. Phys Commun 1981;21(3):421.
[23] Meiboom S, Gill D. Rev Sci Instrum 1958;29:688.
[24] Lorimer JP. In: Mason TJ, editor. Polymers in chemistry with ultrasound. London: Elsevier Applied Science; 1990.
[25] Price GJ. In: Crum LA, editor. Polymer sonochemistry: controlling the structure and properties of macromolecules in sonochemistry and sonoluminescences. Boston: Kluwer Academic Publishers; 1999. p. 321.
[26] Price GJ, Smith PF. Eur Polym J 1993;29:419.
[27] Cassagnau P, Melis F, Michel A. J Appl Polym Sci 1997;65:2395.
[28] Randall D, Lee S, editors. The polyurethane book. New York: Wiley; 2002. p. 171–4.